Tellus (2007), 59B, 470–482
Printed in Singapore. All rights reserved

TELLUS

Experimental assessment of N_2O background fluxes in grassland systems

By ALBRECHT NEFTEL[1]*, CHRIS FLECHARD[1], CHRISTOF AMMANN[1], FRANZ CONEN[2], LUKAS EMMENEGGER[3] and KERSTIN ZEYER[3], [1]*Research Station Agroscope Reckenholz Tänikon (ART) Reckenholzstrasse 191, 8046 Zürich, Switzerland;* [2]*Environmental Geosciences, University of Basel, Bernoullistrasse 30, 4056 Basel, Switzerland;* [3]*Swiss Federal Laboratories for Materials Testing and Research, Ueberlandstrasse 129, 8600 Dübendorf, Switzerland*

(Manuscript received 28 April 2006; in final form 29 January 2007)

ABSTRACT

In the absence of, or between, fertilization events in agricultural systems, soils are generally assumed to emit N_2O at a small rate, often described as the 'background' flux. In contrast, net uptake of N_2O by soil has been observed in many field studies, but has not gained much attention. Observations of net uptake of N_2O form a large fraction (about half) of all individual flux measurements in a long-term time series at our temperate fertilized grassland site. Individual uptake fluxes from chamber measurements are often not statistically significant but mean values integrated over longer time periods from days to weeks do show a clear uptake. An analysis of semi-continuous chamber flux data in conjunction with continuous measurements of the N_2O concentration in the soil profile and eddy covariance measurements suggests that gross production and gross consumption of N_2O are of the same order, and as consequence only a minor fraction of N_2O molecules produced in the soil reaches the atmosphere.

1. Introduction

The exchange of N_2O between ecosystems and the atmosphere depends on complex interactions (see e.g. Williams et al., 1992), with the availability of substrate as the feeding process on one side and the availability of oxygen determining on the other side which pathway is taken in the nitrification or denitrification route. Field experiments have shown an exponential increase of N_2O emissions with increasing water filled pore space (WFPS) up to about 90% when other factors were not limiting (Dobbie and Smith, 2003; Smith et al., 1998). The proportion of emitted N_2O is believed to be greatest at about 80% WFPS (Granli and Bockman, 1994). It is commonly assumed that N_2O respiration (complete denitrification to N_2) occurs under anaerobic conditions ($pO_2 < 0.1\%$) in the open pore space. Such conditions prevail if WFPS exceeds 95%. Net uptake fluxes are therefore expected to occur only for nearly or completely water saturated soils.

A few field studies have discussed observations of net uptake fluxes of N_2O, indicating that consumption dominates production of N_2O (Ryden, 1981; Papen and Butterbach-Bahl, 1999; Schmid et al., 2001). In other studies, uptake fluxes are visible in the presented data but they are not further investigated (e.g. Leahy et al., 2004). N_2O uptake fluxes seem to appear also in conditions when macropores in the soil are well aerated (Chapuis-Lardy et al., 2006). These observations seem to contradict the traditional concept of denitrification in which N_2O respiration dominates production only in anaerobic conditions (Davidson, 1991; Meixner et al., 1997; Potter et al., 1996). However, Arah and Vinten (1995), and Rappoldt and Crawford (1999), already reported the existence of anaerobic aggregates in otherwise well aerated soil where complete reduction of N_2O to N_2 can take place. Oxygen limited sites can develop in well-aerated soil inside aggregates, at locations where the rate of O_2 consumption exceeds the rate of O_2 diffusion (Hojberg et al., 1994; Smith, 1977). These conditions are favoured by large aggregate sizes (Manucharova et al., 2001) and poor connection to macro-pores (Rappoldt and Crawford, 1999).

In this paper, we investigate 'background' fluxes of N_2O and assess the significance and the validity of net N_2O uptake fluxes. Soils with low N input often have N_2O exchange rates close to zero, and this may even be true much of the time for intensively managed soils. When modelling such situations, the question whether soils can be a sink for atmospheric N_2O becomes essential. Models must determine whether the smallest possible value for simulated fluxes is zero or whether uptake fluxes are allowed.

*Corresponding author.
e-mail: albrecht.neftel@art.admin.ch
DOI: 10.1111/j.1600-0889.2007.00273.x

We also address the question to which extent consumption can offset the production.

For the period 2002–2006, we measured with increasing intensity N_2O fluxes using static chamber systems at our CarboEurope and NitroEurope grassland site. In August and September 2005, we made micrometeorological flux measurements at the field scale using a Quantum Cascade Laser Absorption Spectroscopy (QCLAS). The site was also equipped with a membrane tube system (METT) that allowed the monitoring of N_2O concentrations in the air-filled pore space of the soil (Gut et al., 1998).

2. Material and methods

2.1. The experimental site

The Oensingen experimental farm site is located in Central Switzerland (7°44′E, 47°17′N) at an altitude of 450 m a.m.s.l. The site is part of the two large integrated European project networks CarboEurope (http://www.carboeurope.org) and NitroEurope (http://www.nitroeurope.eu). The soil is classified as stagnic cambisol (eutric), with pH = 7.3, Soil organic carbon (SOC) = 27 mg C g^{-1} soil dry matter in the layer 0–30 cm, clay content = 42% and a C/N ratio = 8. Soil porosity measurements indicated an average total pore space of $\varepsilon_0 = 0.56$ m^3 m^{-3} in the soil horizon 0–30 cm, and also showed a bimodal pore size distribution where microporosity (pF > 4.2) accounted for permanent wilting point (Θ_{PWP}) = 0.32 m^3 m^{-3} (58% of ε_0) and macropososity (pF < 2.5) made up another 0.14 m^3 m^{-3} (26% of ε_0). The potential field capacity amounted on average to potential field capacity (Θ_{PFC}) = 0.43 m^3 m^{-3}. The climate is temperate continental, with an average annual rainfall of about 1200 mm and a mean annual air temperature of 9 °C. The study field was until 2000 an 8-yr ley-arable rotation, including summer- and winter-wheat, oilseed rape, maize and bi- or tri-annual grass-clover mix, with an average annual fertilization level of around 110 kg N ha^{-1}. The field was ploughed for the last time in November 2000 and then converted to permanent grassland. The field was divided into two parts, an intensively and an extensively managed field. In May 2001, grass/clover mixtures were sown (seven species on the intensive side). The intensive field was fertilized twice to thrice yearly with cattle slurry and twice yearly (with ammonium nitrate (NH_4NO_3) pellets, altogether amounting to about 200 kg N ha^{-1}. There was no grazing on either field during the study period; both fields were cut mechanically and harvested as hay or silage with varying annual frequencies depending on meteorological conditions, typically 3–4 times a year. In this paper, we concentrate on measurements made on the intensive field. CO_2 and H_2O fluxes were routinely measured with a LICOR 7500/Gill system (Ammann et al., 2007).

Soil temperature was monitored at five depths (2, 5, 10, 30 and 50 cm), while volumetric soil water content (SWC, m^3 H_2O m^{-3} bulk soil) was measured at the four lower depths only, using frequency domain reflectometry (FDR) probes (ThetaProbe ML2x, Delta-T Devices, Cambridge, UK).

2.2. N_2O flux measurement techniques

2.2.1. Chamber measurements. Nitrous oxide fluxes were measured using opaque static chambers (Smith et al., 1995; Conen and Smith, 1998). Four automatic, stainless steel static chambers (L= 300 mm, H = 250 mm), custom built by the Physics Department of the University of Bern, provided flux measurements every 2 hours for 10 min at several locations in the field. The chambers were equipped with a small fan and mounted atop a PVC frame that was driven 10 cm into the soil. Concentrations of N_2O, CO_2 and H_2O in the headspace were determined once per min using an INNOVA 1312 photoacoustic multi-gas analyser (INNOVA Air Tech Instruments, Ballerup, Denmark; www.innova.dk) in a closed loop. Interferences in the measurements are caused by overlaps in the absorption spectra of the different gases and by temperature effects. N_2O concentrations were found to be heavily CO_2- and temperature- dependent, calling for a correction procedure to substitute the algorithm provided by the manufacturers (Flechard et al., 2005). The noise in the resulting corrected N_2O concentration was about 20 ppb for ambient air (typically 370 ppm CO_2 and 320 ppb N_2O), and about 30 ppb for a gas mixture of 2000 ppm CO_2 and 2000 ppb N_2O, which are typical of the static chamber atmosphere after a 10-min closure in warm summer conditions with high soil N_2O emission. The N_2O exchange flux between the soil/vegetation system and the atmosphere is proportional to the change in headspace N_2O concentration (C) over time:

$$F(t) = \frac{V}{A}\frac{\mathrm{d}C}{\mathrm{d}t} = H \cdot \frac{\mathrm{d}C}{\mathrm{d}t}, \tag{1}$$

with V headspace volume, A surface area and H chamber height. In practice, the slope of the linear regression of N_2O concentration versus time was used. A conservative estimate of the N_2O flux detection limit over 10 min is given as:

$$H\frac{\Delta C_{noise}}{\Delta t} = 0.25m\frac{20\,\mathrm{nmol}\cdot\mathrm{mol}^{-1}/0.0224\mathrm{m}^3\cdot\mathrm{mol}^{-1}}{600s} = 0.37\,\mathrm{nmol}\cdot\mathrm{m}^{-2}\cdot\mathrm{s}^{-1} = 16\,\mathrm{ngN_2O}\cdot\mathrm{m}^{-2}\mathrm{s}^{-1}.$$

The regression statistics of CO_2 concentration versus time were used as a quality control criterion. Flux data points were rejected if the regression coefficient (r^2) fell below 0.95, because this indicates for e.g. that the chamber was not properly sealed, or that air samples were somehow contaminated, or the presence of any other significant CO_2 source not due to soil efflux. The calculated N_2O fluxes were corrected for the dilution of the air samples caused by increasing water vapour.

Between two consecutive chamber measurements, ambient air was sampled for 20 min. In order to obtain an estimate of the precision of the flux, the last 10 min of each of these periods were

treated in the same way as a normal chamber measurement, i.e. the slope of the linear regression of N_2O concentration versus time was calculated. Assuming that the ambient N_2O concentration during daytime is constant over time, which is justified when the boundary layer is well mixed, this analysis actually gives an upper estimate of the precision. The 'blank' N_2O fluxes thus simulated gave a mean value of -1.6 ± 1.4 ng N_2O $m^{-2}s^{-1}$ with a standard deviation of 10 ng N_2O $m^{-2}s^{-1}$.

2.2.2. Eddy covariance flux measurements with a quantum cascade laser system.

2.2.2.1. Quantum cascade laser absorption spectroscopy system. Eddy covariance (EC) flux measurements were done using a combination of a sonic anemometer (Gill Solent HS, 20 Hz sampling rate) and a Quantum Cascade Laser Absorption Spectrometer (QCLAS) developed at Aerodyne Research, Inc (Nelson, et al., 2002). The QCLAS was driven with short ($\sim$10 ns) pulses in a 1% duty cycle at -25 °C. Stability of the signal was enhanced by normalizing pulse-to-pulse intensity variations with temporal gating on a single detector. Both laser and detector were thermoelectrically cooled, giving a cryogen-free instrument, which can run unattended for extended time periods.

Samples were measured at 65 mbar in a 0.5 l astigmatic multipass absorption cell with a path length of 56 m. Data acquisition and analysis was done by TDLWintel, a commercially available software package. The program uses spectral parameters listed in the Hitran database (Rothman, et al., 2003) to derive gas concentrations. Absorption spectra at a wavelength of 2241 cm^{-1} were recorded by sweeping the laser across the absorption features at a rate of 5 kHz. Co-averaged spectra were quantified at 5 Hz. Background and reference spectra were measured every 30 min. High purity nitrogen was used for background, and pressurized air as a reference gas. N_2O and CO_2 concentrations of the latter secondary standard were determined in comparison with a CMDL standard (Climate Monitoring and Diagnostics Laboratory, NOAA, USA). While excellent linearity is typically observed for this system, calculated absolute concentrations can differ from the true value by up to 20% if no reference gas is used. In the laboratory, a precision of 0.3 ppb rms (1 Hz) and 1 ppm rms (1 Hz) are typically observed for N_2O and CO_2, respectively. Under field conditions, the corresponding values were determined every 30 min based on measurements of compressed air during 20 s. We found about 0.6 ppb (N_2O) and 2 ppm (CO_2) for the first measurement period, and 0.3 ppb (N_2O) and 1 ppm (CO_2) for the measurements with a new laser.

The spectrometer was located in an air-conditioned trailer, and samples were drawn through 40 m perfluoralkoxy copolymer (PFA) (O.D. $\frac{1}{4}$,′ I.D. 3.5 mm) tubing, the tip of which was attached close to the sonic anemometer. The inlet line and the cell were purged with a flow rate of 6 l min^{-1} resulting in a turbulent flow with a tube residence time (delay time) of about 3 s. Samples were drawn into the cell using an oil-free vacuum pump (Varian Triscroll 300), which leads to a response time of the cell of 0.3 s.

2.2.2.2. Flux calculation and correction of high frequency losses. To calculate the fluxes, we used the EC calculation method described by Spirig et al. (2005). Briefly, a single QCLAS data point is regarded to be representative for the whole time period of the measuring cycle of 0.2 s, while during the same time interval the sonic anemometer (20 Hz) delivers four data points. The QCLAS data thus need to be brought up to the same time resolution of 20 Hz, which is technically implemented by simply repeating the QCLAS concentration of a particular cycle until the next data point is available. After this procedure, similar equidistant time series (time resolution $\Delta t = 0.05$ s) of sonic wind data and QCLAS data are available for the flux calculations. Following the eddy covariance method, the uncorrected vertical flux of a trace gas F_{ECraw} is calculated as the covariance of the discrete time series of the detrended vertical wind w(t) and the detrended concentration c(t) over an averaging period T_a of typically 30 min with τ_{del} representing the time displacement between the vertical wind speed and the scalar:

$$F_{\mathrm{ECraw}} = \mathrm{cov}_{\mathrm{wc}}(\tau_{\mathrm{del}}) = \left(\frac{\Delta t}{T_a}\right) \cdot \sum_{t=0}^{T_a} w(t) \cdot c(t - \tau_{\mathrm{del}}). \qquad (2)$$

The two time series are adjusted to each other by a delay time that accounts for the residence time in the air sampling tube and possible time difference between the data acquisition systems. The time delay was calculated for each measuring interval separately by determining the maximum in the covariance function of the CO_2 flux. In cases where no clear maximum could be found within the physically possible limits of the lag, an interpolated best guess for the lag was used. The data treatment, the inlet tube and the separation distance between the sampling tube inlet and the anemometer sensor led to a damping of high-frequent turbulent fluctuations of the trace gas concentrations before the detection by the QCLAS. We developed an empirical correction approach using the spectral information of the measured flux time series, i.e. the flux 'ogives' and comparing it to the corresponding time series of the heat flux calculated from the sonic temperature that experienced almost no damping (Ammann et al., 2006). The ogive is defined as the cumulative sum of the finite co-spectrum.

The QCLAS measurements are sensitive to the absolute trace gas density. Since water vapour was not removed from the sample air to keep the set up simple, a correction for the density fluctuations due to the water vapour flux must be applied (Webb et al., 1980), commonly named Webb, Pearman and Leuning (WPL) correction. A correction due to the sensible heat flux can be omitted because the long inlet line damped the air density fluctuation associated with the sensible heatflux. The WPL corrected flux is given by the following equation:

$$F_{\mathrm{WPLcorr}} = F_{\mathrm{ECraw}} + \overline{c} \cdot F_{\mathrm{H2O}}$$
$$(\mathrm{c\ in\ mol\ mol^{-1}\ and\ F_c{'}s\ in\ m\ s^{-1} \cdot mol\ mol^{-1}}). \qquad (3)$$

2.2.3. Membrane tube technique (METT) system. Additional insight into soil processes controlling N_2O fluxes was provided by concurrent measurements of soil pore space N_2O and CO_2 concentrations using the METT technique (Gut et al., 1998; Schmid et al., 2001). Hydrophobic, gas-permeable porous polypropylene tubes (Accurel® PP V8/2) were installed permanently in May 2001 at five depths (2, 5, 10, 30 and 50 cm), allowing a gaseous equilibrium to be maintained between soil pore space and the tube interior. A second INNOVA 1312 analyser was used for trace gas determination. Sampling was done sequentially for 10 soil tubes (five depths on both fields) plus one additional tube placed at the soil surface and an inlet line for ambient air at 1 m above ground. During each step (10 min.) of the overall cycle (120 min.), sample air was circulated in a loop between the tube and the analyzer, except for ambient air (Flechard et al., 2007).

3. Results

3.1. Static chamber fluxes

The analysis presented in this paper is based on measurements made from January to October 2005 on the intensively managed grassland field. Figure 1 shows an overview of all fluxes measured with automated static chambers. The data shows the typical pattern of N_2O emission from fertilized agricultural plots: the peaks are associated with the application of fertilizers and last only a few days. Individual fluxes after fertilizer application can vary rapidly and also spatially as fluxes close to zero in one chamber can coexist with high fluxes recorded in another only a few meters away on the same field. (e.g. first half of April 2005). Between fertilizer events, fluxes were most of the time below 100 ng N_2O $m^{-2}s^{-1}$ and were scattered around zero. Uptake fluxes up to -90 ng N_2O $m^{-2}s^{-1}$ were observed. The largest uptake fluxes were measured in dry conditions with soil temperature between 15 °C and 25 °C. For background fluxes there was no discernable systematic dependence on either WFPS or temperature, contrary to the expectation that uptake fluxes should be enhanced by anaerobic conditions in the soil that are favoured by high WFPS.

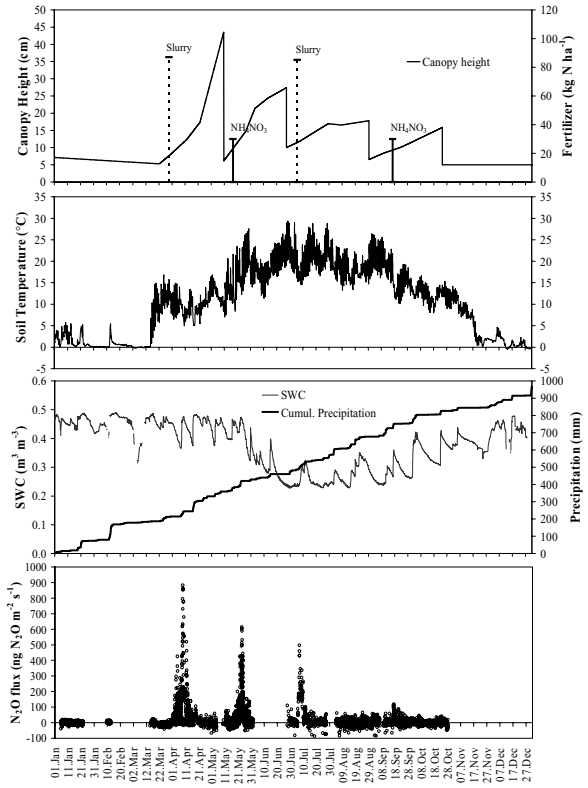

Fig. 1. Overview of N_2O chamber measurements of the year 2005. Canopy height together with fertilizer applications, soil temperature (5 cm depth) and soil water content (5 cm depth) are indicated. Chamber data have a resolution of two hours, soil temperature and soil water content are 30 min average values.

The original aim of the chamber measurements was to determine the annual cumulated N_2O flux (Flechard et al., 2005). In total, four automated chambers were available and their distribution between the extensive and intensive field varied throughout the year. The intensity of the measurements increased around events such as cuts and fertilization. Therefore, there may be a bias in chamber allocation to a given field towards emission fluxes due to the application of more than two chambers on the same field to catch such specific emission events. An analysis of all two-hr periods when two to four chambers were in operation on the intensive grassland field shows that a consistent uptake flux of all chambers on the same field is more the exception than the rule and is statistically compatible with a net zero flux. In contrast, emission peaks are often seen simultaneously in all chambers. Of all cases when two chambers were operated on the same field, 31% showed a net uptake flux in both chambers and 24% showed an emission in both chambers. Out of 276 two-hour cycles where three chambers operated in parallel, 6.5% consistent uptake and 48% consistent emission were recorded. Finally out of the 221 cycles with four chambers, the percentage with consistent uptake was only 2.7% while 44% showed emission in all four chambers.

3.2. Eddy covariance fluxes

The QCLAS system was operated in August and September 2005. The measuring period consists of two continuous datasets with a break caused by a failure of the laser. A rigorous selection of the EC data was applied in order to retain only cases where a flux could clearly be identified and be related to the grassland field, as indicated with quality index q0 (Fig. 3b, full triangles). The selection criteria required that the CO_2 flux had a monotonic increasing ogive function and that the contribution in the low frequency range ($T_{period} > 500$ s) was below 30%. Although this rejection criterion is somewhat arbitrary, it has the merit of eliminating flux values that are strongly affected by advection.

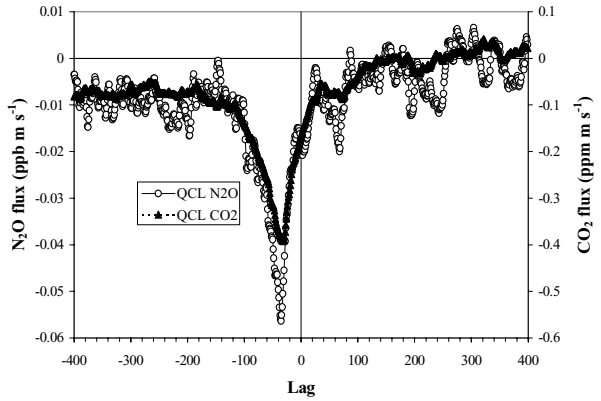

Fig. 2. Covariance function on August 18th 12:30–13:00 of CO_2 and N_2O flux (QCLAS system). One lag unit corresponds to a shift of 0.05 s between the two correlated time series.

For the remaining data, only a likely range of the flux can be given. Figure 2 shows an example of the covariance function with easily identifiable peaks that correspond to the CO_2 and N_2O fluxes. The lag of -35 steps corresponding to a time shift of 1.75 s is given by the delay between the measurement of the vertical wind speed and the concentration measurement by the QCLAS. No corrections were applied to the covariance functions shown in Fig. 2.

Beside the clear peak, distinct structures are visible in the covariance function that exceeds random noise. Reasons for such structures may be due to non-ideal instrumental noise as well as advection effects. The error indicated for the q0 fluxes (error bar with solid line) and the range for the rejected data (dashed line) were calculated as the standard deviation of the covariance function of the vertical wind and the N_2O concentration (eq. (2)) far outside of the true time lag ($-1200 < \tau_{del} < -800$ and $800 < \tau_{del} < 1200$; τ_{del}: number of points, corresponding each to a time delay of 0.05 s), as first proposed by Wienhold et al. (1995). This error approach takes into account variations in the covariance function that potentially disturb the flux determination. It is an estimate at the high end, because it assumes that the covariance is ideally zero in the considered lag range.

The data shown in Fig. 3 cover a typical background emission phase where both chamber and EC fluxes were bound in a narrow range between +50 and −40 ng N_2O $m^{-2}s^{-1}$. The mean chamber flux over the period shown in Fig. 3 was -5.5 ng $\pm$ 2.6 (95% confidence interval) N_2O $m^{-2}s^{-1}$ with a standard deviation of 17.4 ng N_2O $m^{-2}s^{-1}$. By comparison, the mean EC flux was 13.9 $\pm$ 4 ng N_2O $m^{-2}s^{-1}$ with a standard deviation of 27 ng N_2O $m^{-2}s^{-1}$ and indicated a small net emission at the field scale.

Figure 4 shows the uncorrected EC flux data together with the WPL correction, as well as the WPL-corrected data, for the first four days of Fig. 3, where in a few cases reliable net uptake fluxes were measured. The indicated uncertainty range is calculated by the Gaussian law of error propagation assuming the above-

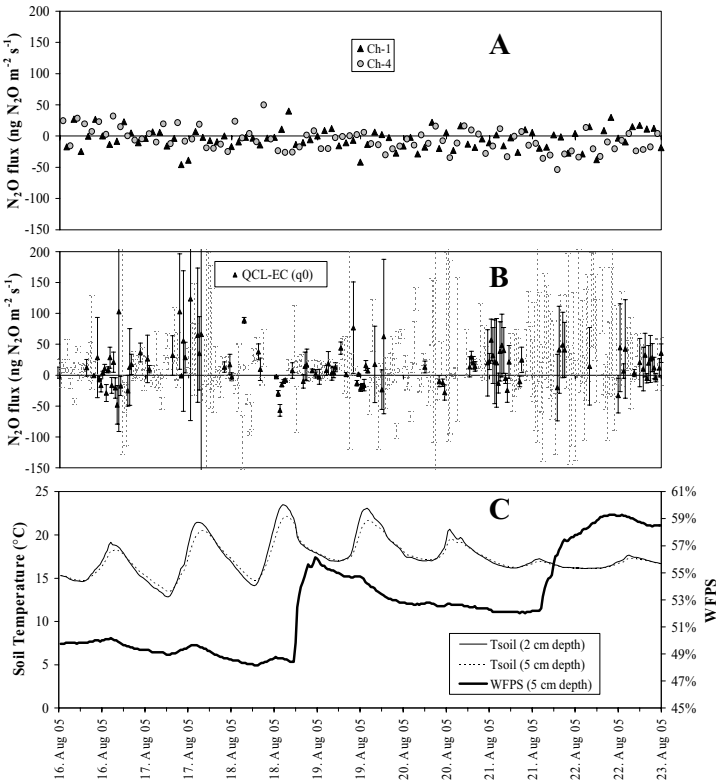

Fig. 3. Field scale QCLAS N_2O flux measurements and chamber data for background conditions in August 2005. A: Chamber fluxes; B: QCLAS-EC fluxes; solid triangles are fluxes that passed the applied quality criteria, broken lines indicate the range of fluxes based on the fluctuation of the covariance function; C: Soil temperature at 2 and 5 cm depth and soil humidity (water filled pore space) at 5 cm depth.

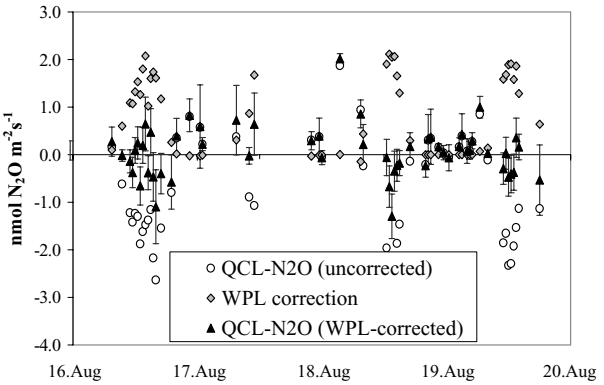

Fig. 4. Eddy covariance N_2O fluxes over a four day period within the period shown in Figure 3. The flux values are shown, together with the WPL correction derived from the water flux measurements and the WPL corrected values. All fluxes are corrected for the high frequency losses. For comparison purposes, N_2O fluxes are also indicated in nmol $m^{-2}s^{-1}$.

described Wienhold error for the QCLAS N_2O measurements and a precision of the WPL correction of $\pm 20\%$. During daytime conditions, EC water vapour fluxes were in the order of several mmol $m^{-2}s^{-1}$ and therefore the applied WPL correction was in the same order of magnitude as the uncorrected EC N_2O fluxes

In the example data shown in Fig. 5, mineral fertilizer was applied and as a consequence a peak N_2O emission event was recorded. The chambers showed an immediate but small response to the application of the fertilizers, declining after two days. As frequently observed (e.g. Ball et al., 1997), the scatter between the individual chambers was large, indicating a large spatial variability. The EC data also showed a clear peak with a maximum, the day after the fertilizer application. The EC flux was on average a factor three higher than the flux recorded with the chambers.

3.3. Soil concentration profiles

The information from the membrane tube system provided independent information about the direction and magnitude of the net N_2O exchange. A simple concept to simulate trace gas flux between soil and atmosphere uses this information on vertical soil concentration gradients coupled with a soil transport coefficient K assuming Fick's law:

$$F = -K \cdot \frac{\Delta c}{\Delta z}. \tag{4}$$

Simultaneous measurements of CO_2 concentrations in soil air-filled pore space and of soil respiration allow an estimate of the transport coefficient that relates the flux with the concentration gradient. Soil CO_2 efflux was measured over a whole year

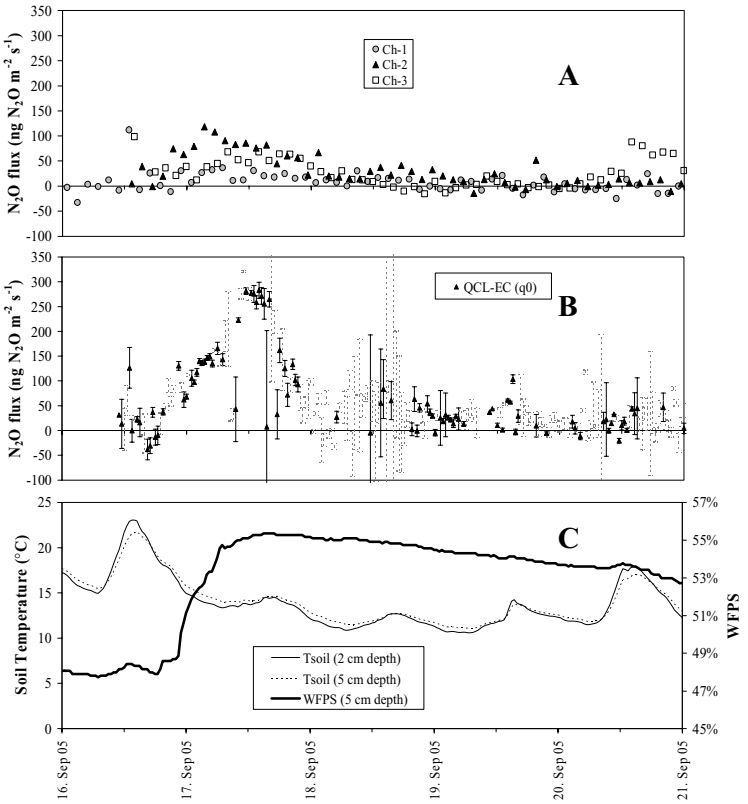

Fig. 5. Field scale QCLAS N_2O flux measurements and chamber data after application of fertilizer in September 2005. A: Chamber fluxes; B: QCLAS-EC fluxes; solid triangles are fluxes that passed the applied quality criteria, broken lines indicate the range of fluxes based on the fluctuation of the covariance function; C: Soil temperature at 2 and 5 cm depth and soil humidity (water filled pore space) at 5 cm depth.

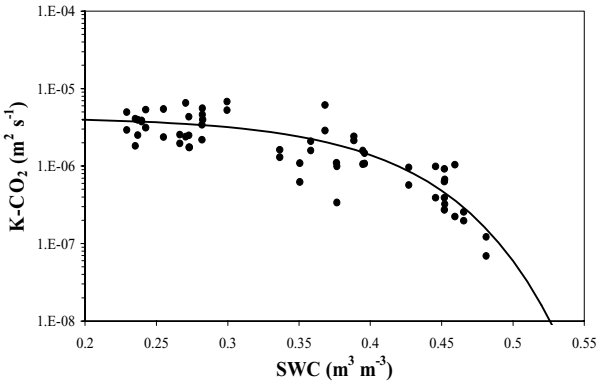

Fig. 6. Evaluation of soil transport coefficient K as a function of soil water content.

using a Li-Cor 6400 soil cuvette (Li-Cor, Lincoln, NE, USA). The K values thus obtained for CO_2 were in the range $1 \cdot 10^{-7}$ $m^2 s^{-1}$ to $3 \cdot 10^{-6}$ $m^2 s^{-1}$ and decreased over-proportionally with increasing SWC (Fig. 6). These values are in the same range as calculated from other models relating soil diffusivity to the water filled pore space (e.g.Millington, 1959; Schüssler, 1996). An empirical parametrization of K as function of soil moisture was developed using a Gompertz sigmoidal fit (Fig. 6) such that:

$$\frac{K}{D_{CO2}} = a * \exp^{[-\exp^{(-k*(1-WFPS-x_c))}]}, \quad (5a)$$

with WFPS, the dimensionless water-filled pore space defined as:

$$WFPS = \frac{SWC}{TPS}, \quad (5b)$$

where D_{CO2} is the molecular diffusion of CO_2 in air ($1.45\ 10^{-5}$ m^2 s^{-1}), TPS the total pore space (0.57 m^3 m^{-3} at our site) and the fitted Gompertz parameters $a = 0.29$, $k = 7.64$, $x_c = 0.31$.

Assuming a similar source/sink distribution for N_2O and CO_2 in the soil profile, the vertical N_2O gradient was combined with the K values derived from CO_2 measurements to simulate the N_2O flux. For example, in Fig. 7, the daily-averaged concentration difference between the soil tube at 2 cm depth and ambient air is plotted in parallel with daily-averaged chamber fluxes for a 2 weeks period in March 2005, during which chamber fluxes showed consistent N_2O uptake. From 20th March through 27th March subambient N_2O concentration were measured at 2 cm depth, but before and after this period soil concentration was actually above ambient concentration. The N_2O fluxes simulated using Fick's law were bi-directional and one order of magnitude smaller than the measured fluxes.

Another case study is shown in Fig. 8, which provides indirect evidence that an efficient consumption mechanism occurs near the soil surface. Following the application of mineral fertilizer on May 17th 2005 at 13:00 central european time (CET) a very high N_2O concentration evolved in the open pore space

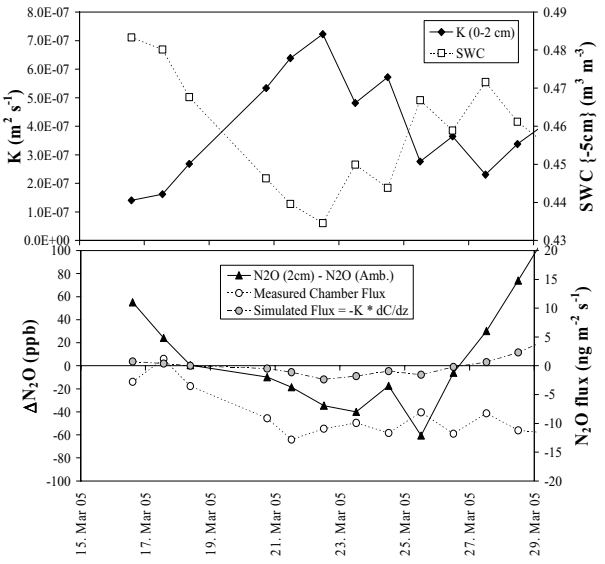

Fig. 7. Estimated variations of soil transport coefficient K (top), N_2O concentration difference between ambient and 2cm soil depth, together with measured and simulated exchange fluxes (bottom). All values are daily arithmetic means.

in the morning of the following day. The concentration at 2 cm depth started to increase early in the morning of May 18th after a light rainfall of 5 mm and reached a first maximum of 66000 ppb around the following midnight. A second peak occurred on the following day in the afternoon and then the concentration dropped again to almost ambient levels within the next 10 hr. The WFPS was around 80% representing optimal conditions for N_2O production. The exchange fluxes measured with four automated chambers installed in the vicinity of the membrane tubes started to slightly increase only on May 19th and fully developed only 3 d later again after a slight rainfall and favoured by warmer soil temperature. WFPS remained on the same level until 26th of May and started to drop afterwards. The high N_2O concentrations measured at 2 cm depth from May 18th to May 20th did not translate into high chamber fluxes. Substantial N_2O emissions occurred only in the later phase (May 20th to May 25th). The simulated (Fick's law) fluxes essentially follow soil N_2O concentration, with a first peak around May 19th and a second much lower peak around May 22nd, with little correlation to the actual fluxes measured by chambers. Both examples shown in Fig. 7 and 8 indicate that the simple diffusion approach is invalid for N_2O, even when limited to the uppermost 2 cm of the soil.

4. Discussion

4.1. Net uptake fluxes – fact or artefact?

4.1.1. Chamber measurements. In the absence of triggering events, soil/atmosphere exchange of N_2O was confined to a narrow range of fluxes from -50 to $+50$ ng N_2O $m^{-2} s^{-1}$, with

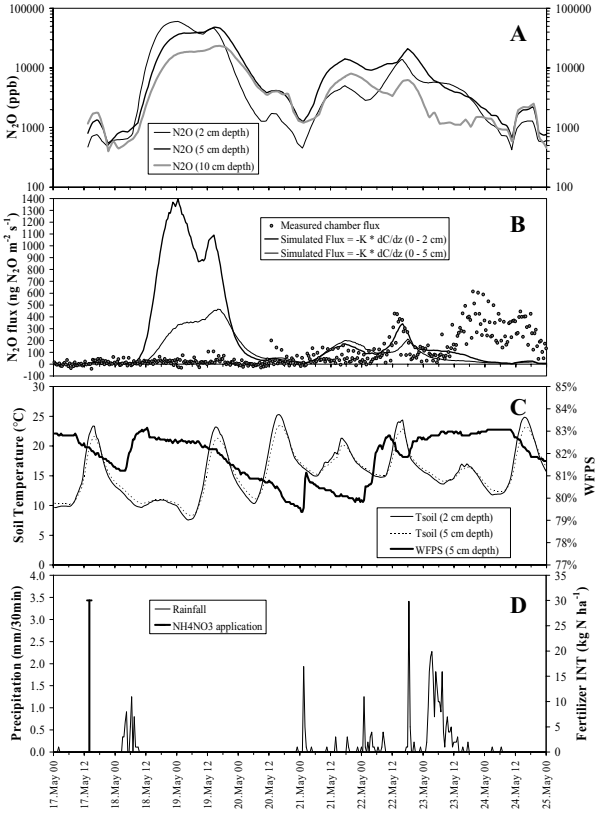

Fig. 8. An example of a strong N_2O concentration peak in the soil as reaction to the application of fertilizer, where N_2O is partly consumed before it reaches the surface. A: Soil concentrations, B: Chamber fluxes and simulated diffusion flux, C: Soil temperature and water filled pore space, D: Precipitation.

roughly two thirds of all measured fluxes not exceeding in absolute value the rather conservative flux detection limit of 16 ng N_2O $m^{-2}s^{-1}$. Surprisingly, flux rates in background conditions seemed to be independent from soil humidity and soil temperature. Such behaviour raises concerns regarding the ability to distinguish small-observed fluxes from noise and whether they can be statistically distinguished from a net zero flux. Regarding the automated chambers, our flux detection limit is higher than indicated in many other reports (Pihlatie et al., 2005; Rosenkranz et al., 2005), mainly due to two reasons: a) the chambers were closed only for 10 min to minimize disturbance of the ecosystem; b) the used analytical system (Innova photoacoustic instrument, model 1312) has at best a precision of ±20 ppb for a single N_2O concentration measurement (Flechard et al., 2005). This lack of precision is however partly compensated by the continuous monitoring of CO_2/N_2O in the headspace of the chamber, so that 9 to 10 concentration measurements are available per flux measurement, which increases the precision of the slope. The rejection of fluxes based on the coefficient of determination for the regression of CO_2 versus time was used because CO_2 respiration fluxes are always detectable. This quality control criterion ensures that the change in N_2O concentration in the headspace adequately reflects the N_2O exchange flux. More than 90% of the uptake flux measurements above 50 ng N_2O $m^{-2}s^{-1}$ have a statistically significant slope below zero (95% confidence level of the linear regression slope). We are therefore confident that cumulated net uptake fluxes over time periods of several days to weeks are not the result of measurement artefacts.

4.1.2. Precision of EC measurements. The flux standard error resulting from (ideal) instrumental noise of the trace gas analyser can be expressed as the product of the standard deviation of the vertical wind (σ_w) and of the noise in the trace gas concentrations ($\sigma_{c,noise}$) divided by the square root of number of independent measurements (N) within the flux averaging interval (Edwards et al. 2003; Pihlatie et al., 2005):

$$F_{SE} = \frac{\sigma_w \cdot \sigma_{c,noise}}{\sqrt{N}}. \quad (6)$$

We consider this error to be a lower limit of precision that is taking into account all sources of uncertainty for field measurements and data treatment. Pihlatie et al. give a detection limit of 4 ng N_2O $m^{-2}s^{-1}$ for a 30 min interval. This is very similar to what we obtain using eq. (6), but about a factor three lower than using the approach by Wienhold.et al. (1995). It should be noted, that the noise of N_2O analysis calculated for 1 Hz time resolution was similar in the above mentioned studies with <2 ppb (Edwards et al.), 0.3 ppb (Wienhold), 0.3 ppb (Pihlatie et al.) and 0.3–0.6 ppb (this study).

Figure 9a shows an exemplary covariance functions for the CO_2 and the N_2O flux obtained by QCLAS for a 30 min interval during night time (03:30 – 04:00) on August 21st. The

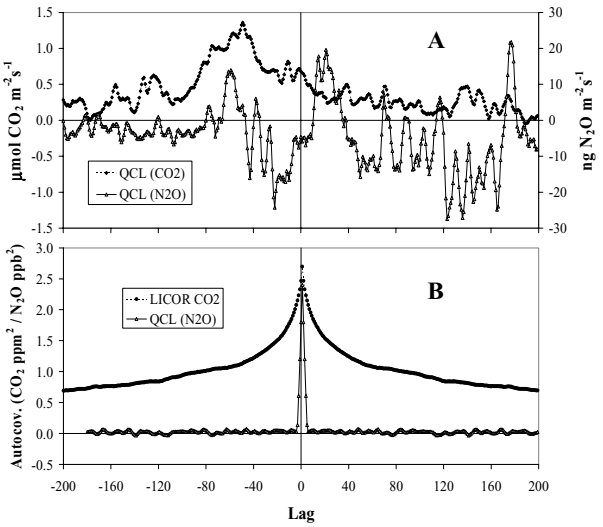

Fig. 9. A: Covariance function of: CO_2 flux measured with LICOR 7500, QCLAS N_2O flux and CO_2 flux on August 21st, 03:30. B: Autocovariance function of LICOR CO_2 concentrations (left y-axis) and QCLAS N_2O concentrations (right y-axis). One Lag unit corresponds to a shift of 0.05 s.

friction velocity for this measurement was 0.28 ms^{-1}, an unusually high value for nighttime conditions at the Oensingen site. Such windy nights allow reliable EC measurements with very low water vapour fluxes and thus very small WPL corrections. The clearly detectable CO_2 flux allows a precise determination of the time lag between the anemometer time series and the QCLAS data. The calculated N_2O flux value is 4 ng N_2O $m^{-2}s^{-1}$ but the N_2O covariance function shows only noise-like variations within a range of $\pm$20 ng N_2O $m^{-2}s^{-1}$. The absolute value of the turbulent flux must be within this range, but cannot be quantified more accurately.

An analysis of the autocovariance function of the QCLAS N_2O concentration time series supports the Wienhold approach for the uncertainty analysis. The autocovariance function A_c of a concentration time series c(t) as defined below offers an additional possibility to assess the noise structure of the EC measurements:

$$A_c(\tau_{\mathrm{del}}) = \left(\frac{\Delta t}{T_a}\right) \cdot \sum_{t=0}^{T_a} c(t) \cdot c(t - \tau_{\mathrm{del}}) \tag{7}$$

The N_2O autocovariance shown in Fig. 9b is not distinguishable from a white noise series, thus completely uncorrelated for any lag greater than 0.2 s, which corresponds to the time resolution of the QCLAS. The standard deviation of the N_2O concentration measurement is 1.6 ppb (1 Hz), which is three times higher than the typical 0.6 ppb (1 Hz) obtained from a gas cylinder each hour in the field. The error calculated from eq.(6) is 4.5 ng N_2O $m^{-2}s^{-1}$ compared to the standard deviation of 10 ng N_2O $m^{-2}s^{-1}$ of the covariance function. For comparison, the autocovariance function of the LICOR CO_2 measurements is added to Fig. 9b. With increasing lag the auto-covariance function smoothly decreases as must be expected for a turbulent exchange process where the different eddies of various sizes have certain persistence. In case, the eddies should carry a measurable N_2O flux a similar persistence would be expected in the N_2O autocovariance function.

The, 'exact' value of 4 ng N_2O $m^{-2}s^{-1}$ that we obtained with the lag defined from the analysis of the CO_2 flux is clearly below the Wienhold error of 20 ng N_2O $m^{-2}s^{-1}$ and should not be regarded as a flux significantly different from zero.

4.1.3. EC measurements of the emission peak after fertilization application. The temporal variations observed with the EC and the chambers are similar in Fig. 5. They are modulated by soil temperature and the WFPS. The fertilization occurred on September 16th at noon when the soil temperature was over 20 °C. The WFPS was below 50%, thus not optimal for N_2O production. In the evening a cold front arrived causing rain and a sharp temperature drop. The increasing water content in the soil stimulated the production and more than compensated the negative effect of soil cooling.

EC measurements integrate over a much larger area (the so-called footprint area) than chambers. It can therefore be expected that the temporal variability for well-defined flux situations, such as emissions after application of fertilizers, should be less than that of chamber measurements that are confined to an area of only 0.09 m^2. On this small scale, distribution of the fertilizer will be inhomogeneous and spatial variability up to a factor of three or more has to be expected. Figure 5 shows this behaviour, even though the magnitude of the fluxes was small due to the rather cold weather. It has to be recognized that chamber measurements and EC measurements can generally not validate each other because they are representative of very different surface scales.

4.1.4. EC background fluxes. The data measured in August 2005 (Fig. 3) were typical of background conditions. For this period the mean EC flux was slightly positive at 13.9 $\pm$ 4 ng N_2O $m^{-2}s^{-1}$, while the mean chamber flux indicated a small uptake statistically barely different from zero (-5.5 ng N_2O $m^{-2}s^{-1}$ $\pm$2.6 ng N_2O $m^{-2}s^{-1}$), which again raises the issue of the comparability of chamber and EC fluxes. The field might be assumed to be made up of a few hotspots of N_2O emission with a combined flux that slightly more than outweighs the combined uptake rate of the rest of the field. In this case the field scale flux as measured by EC will be slightly positive, whereas the probability to capture a representative sample of the field's flux distribution with only a handful of chambers is fairly low. A likely outcome is that the mean chamber flux will be slightly negative because no hotspot was sampled.

WPL-uncorrected EC fluxes in Fig. 4 show pronounced diurnal variations that are strongly correlated with the water vapour flux. The largest fluxes reach more than -120 ng N_2O $m^{-2}s^{-1}$ at midday. Applying the WPL correction brings most of the fluxes close to zero. Only a few significant uptake fluxes remain, and even in these cases the applied WPL correction is larger than the remaining N_2O flux, implying that net uptake fluxes are very difficult to measure using EC with the current setup. It is interesting to note that during the measuring period of Fig. 3 significant uptake fluxes were only observed during daytime.

4.2. *Comparison of surface fluxes and soil concentrations*

The quasi-continuous measurements of the below-ground N_2O concentrations in the open pore space delivers a qualitative insight into the dynamics of production and consumption processes of N_2O. A net uptake can be expected if the concentration in soil open pore space close to the surface is below the ambient concentration. Fick's law (eq. (4)) is the simplest approach to estimate the flux from the concentration difference between soil and the atmosphere under the assumption of a constant flux through the layer of the thickness Δz and a negligible source in this layer.

During periods when daily mean chamber fluxes show a net uptake of N_2O, concentrations in the soil were only part of the time below the atmospheric concentration. The concentration gradient between the atmosphere and the open pore space at a depth of 2 cm in the soil reaches 50 ppb at most (Fig. 7). The

expected uptake fluxes under the assumption of Fick's law, and using the evaluated transport coefficient K are roughly one order of magnitude smaller than the measured ones. This discrepancy suggests that the uptake of N_2O takes place in a very shallow surface layer. This is the reason why concentrations at depths greater than 1–2 cm cannot be used to evaluate N_2O fluxes. We assume that the concentration difference between soil and atmosphere measured at a depth of −2 cm is already established after a few mm. As a consequence the soil concentration at −2 cm would represent a compensation point where consumption and production processes are in equilibrium with a scale length (z_{eff}) of below 1 cm (Neftel et al., 2000).

This concept is well known for NO (Galbally and Johansson, 1989). The determination of the compensation concentration (i.e. the concentration in the soil where consumption equals production) in the laboratory has been successfully used to evaluate the potential emissions of soil samples from different locations in a standardized manner (Meixner et al., 1997; Gut et al., 1999). The laboratory measurements show that consumption of NO can be described by a first order process, characterized by a simple rate constant.

Assuming homogeneous conditions in the soil and a first order uptake mechanism (i.e. the consumption process is proportional to the concentration) an uptake rate is defined as:

$$R_{\text{uptake}} = \frac{K}{(z_{\text{eff}})^2} \tag{8}$$

The uptake rate is the time constant characterizing the first order mechanism. With a range of the transport coefficient of $2–10 \cdot 10^{-7}\ m^2 s^{-1}$ and a hypothetical scale length of 1 cm the corresponding range of the uptake rate is between $2–10 \cdot 10^{-3}\ s^{-1}$.

The rather high soil water content corresponding to a WFPS around 80% during the period shown in Fig. 7 suggests that the water phase plays an important role in the uptake process. Atmospheric N_2O molecules might be taken up at the surface into the water phase and then be transported to microbes where they are further reduced to N_2.

Figure 8 shows a mirror image of the situation presented in Fig. 7. The very high peak is obviously caused by rain after mineral fertilizer was applied. The first peak occurring in the soil concentration during the night from May 18th to May 19th did not translate into an emission peak in any of the four chambers that were in operation on the same field, contrary to the expectation that N_2O molecules would diffuse through the 2 cm soil layer into the atmosphere. The N_2O molecules that were produced and emitted into the macropore space at 2 cm depth never reached the surface. WFPS at −5 cm recorded during this event was around 80% thus in the optimal range for N_2O production. Soil diffusivity deduced from the CO_2 flux gradient ratio was of the order of $2 \cdot 10^{-7}\ m^2 s^{-1}$. The corresponding diffusion time through a 2 cm layer is 2000 s. The lifetime of N_2O molecules must therefore be shorter than this value. With the same principles as assumed in the previous paragraph a rate constant of $5 \cdot 10^{-4} s^{-1}$ or faster is deduced. This is in the same order of magnitude as derived in earlier investigations in a similar soil (Neftel et al., 2000).

4.3. Mechanisms of N_2O uptake in the soil

If we accept that the reduction of N_2O to N_2 is a microbial and anaerobic process, our data suggest that in the soil anaerobic spots exist in an otherwise aerobic environment. Microbiological processes take place within living cells, on their membranes, or within the environment into which enzymes are released. Various limitations restrict microbial life and expansion (Ekschmitt et al., 2005) so that less than 5% of the overall available space is colonised by active microorganisms at any one time (Nannipieri et al., 2003). Cells and exo-enzymes perform their reactions only in solution or when covered by a film of water. Low solubility of O_2 in water and large O_2 demand in biofilms covering organic residues can result in anaerobic conditions under less than 200 μm of water (Dalsgaard et al., 1995; Parkin, 1987). Similarly, reduction in O_2 concentration from nearly atmospheric to zero within a few millimetres have been observed in soil clods (Sextone et al., 1985; Hojberg et al., 1994; Rappoldt, 1995; Sierra et al., 1995), whereby these measurements probably integrated across the liquid phase of biofilms and the gas phase of micropores. In such environments, denitrifiers are able to use oxidised N molecules as electron acceptors. A large variety of the soil microbial population is able to denitrify several or all forms of oxidised N, such as NO_3^-, NO_2, NO and N_2O (Zumft, 1997).

The solubility of N_2O in water is about 20 times greater than for O_2. Hence, from the microbial perspective, N_2O is much more readily available than may seem from its concentration in air-filled pore space. Still, rates of reduction of atmospheric N_2O will always remain very small because of the diffusion limitation. In contrast, N_2O emission from sites with abundant NO_3^- or NO_2^- supply is mainly limited by the rate of N_2O production and little by diffusion. Therefore, rates of N_2O emission can be much larger than rates of N_2O uptake. Measurements integrating over a large number of sites, in which the large majority constitute small net N_2O sinks, and only a few sites constitute larger net N_2O sources, will more often indicate net N_2O emissions.

The membrane tubes must be regarded as an additional 'dry' macropore, and the measured concentration is that of soil macropores, which make up only about 26% of the total pore space (Flechard et al., 2007). Our dataset gives ample evidence that consumption processes do occur under conditions where oxygen concentration in the macropores is only marginally depleted. A mechanism is needed to create local anaerobic conditions around the denitrifiers. The autotrophic and heterotrophic respiration associated with the microbial activity is likely to depress locally the oxygen content. On the field scale significant uptake fluxes measured by EC have only been observed only during daytime.

Table 1. Reported activities of N_2O sink in studies where at least part of the observed sink was statistically significant

Location (Reference)	Ecosystem and management	Duration of study (years)	Duration of net sink activity (fraction of study period)	Mean N2O sink during sink period (nmol m^{-2} s^{-1})
Berkshire, UK (Ryden, 1981)	Grassland, no fertiliser N	0.3	1.00	0.05
	Grassland, 250 kg N year-1	0.7	0.46	0.11
Bolívar State, Venezuela (Donoso, 1993)	Undisturbed savannah, dry season	0.1		0..04
Eastern Amazonia, Brazil (Verchot et al., 1999)	Pasture, active	1.3	0.13	0.06
	Pasture, degraded	1.3	0.19	0.02
Black Forest, Germany (Papen et al. 2001)	Spruce forest, control	2.4	0.56	0.02
	Spruce forest, N-fertilised	2.4	0.33	0.02
Swiss Plateau (Flechard) (et al. 2005)	Extensive grassland, no fertiliser N	2.5	0.7	0.11

Therefore we may speculate that plant activity also plays an important role. During active photosynthesis, more readily available C can be discharged by the roots (Murray et al. 2004), stimulating respiration and leading to local oxygen depletion with subsequent consumption of N_2O.

4.4. Significance of the N_2O uptake for the global budget

The global atmospheric N_2O budget is assumed to be reasonably well understood, with the estimated source ranges covering the estimated range of the stratospheric loss (Houghton et al., 1996; Yoshida and Toyoda, 2000). Galloway et al. (2004) assume a value of 10 Tg N yr^{-1} for both natural and anthropogenic soil sources. The global vegetated surface area is about $12 \cdot 10^{13}$ m^2. Hence, mean emissions are equivalent to about 0.09 nmol m^{-2} s^{-1}. (= 4 ng N_2O m^{-2} s^{-1}), but the estimated range of the contribution of agricultural soil (0.6–14.8 Tg N yr^{-1}) is very large (Houghton et al., 1996). This range reflects the large variability of the measurements. Table 1 summarizes studies that reported statistically significant net N_2O uptake over longer time periods.

These studies report an uptake activity on average over half the observation period. Mean uptake rates ranged from 0.02 to 0.11 nmol $m^{-2}s^{-1}$. Most field studies so far were done on systems subject to agricultural N input or land use change. These two compartments constitute major and growing sources of N_2O. Thus, it is not surprising that reports where net N_2O uptake have been treated in detail are rare and it is therefore difficult to estimate the global importance of the uptake. We might speculate that half of the total vegetated area takes up N_2O for half of the year at a rate of 0.06 nmol m^{-2} s^{-1}, the mean value in Table 1 (see also Conen and Neftel, 2007). This would be equivalent to about 20% of the total current estimated soil N_2O source. Bange (2006) suggest an upward revision of the global oceanic N_2O source of at least a factor 2 from a range of 1–5 Tg N yr^{-1} to 2–10 Tg N yr^{-1}. As a consequence, either the terrestrial source would need to decrease by the same amount, or an additional sink is present in case the stratospheric sink remains unchanged. The net N_2O uptake by soils is potentially strong enough to compensate the proposed increase of the oceanic source.

5. Conclusions

Small-observed net uptake fluxes point to a widespread consumption process of N_2O in the soil taking place in anaerobic niches that are present in an otherwise aerobic environment. The N_2O consumption process might be described by a first order uptake mechanism with a rate constant in the order of 10^{-3} to 10^{-4} s^{-1}. As a consequence, the gross production of N_2O could be estimated from time series of N_2O concentration measurements in the open pore space in the soil. It is likely that about 80 to 90% of the N_2O produced in the soil is reduced to N_2 and that this pathway is a substantial part of the N-cycle in soils. Galloway et al. (2004) estimate that on a global scale the ratio of produced N_2 to N_2O of about 7. It is well known that denitrification produces a mixture of N_2O and N_2, where N_2 is the result of complete reduction during the process. In addition, a large proportion of N_2O seems to be reduced while diffusing through the macro-pore space towards the soil surface.

6. Acknowledgments

We are grateful to two anonymous reviewers, whose careful and detailed reviews substantially improved the manuscript. This study was supported by the Swiss State Secretariat for Education and Research through grant Nr. C04 0254 to COST Action 856 and through grant Nr. SBF Nr. 03.0350-1 Carbo Europe-IP (GOCE-CT-2003–505572).

References

Ammann, C., Brunner, A., Spirig, C. and Neftel, A. 2006. Technical note: Water vapour concentration and flux measurements with PTR-MS. *Atmos. Chem. Phys. Discuss.* **6**, 5329–5355.

Ammann, C., Flechard, C., Leifeld, J., Neftel, A. and Fuhrer, J. 2007. The carbon budget of newly established temperate grassland depends on management intensity. *Agriculture, Ecosystems and Environment*. doi:10.1016/j.agee.2006.12.002.

Arah, J. R. M. and Vinten, A. J. A. 1995. Simplified models of anoxia and denitrification in aggregated and simple-structured soils. *European J Soil Sci.* **46**(4), 507–517.

Ball, B. C., Horgan, G. W., Clayton H. and Parker, J. P. 1997. Spatial variability of nitrous oxide fluxes and controlling soil and topographic properties. *J Environ. Qual.* **26**, 1399–1409.

Bange, H. W. 2006. New Directions: The importance of oceanic nitrous oxide emissions. *Atmos. Environ.* **40**, 198–199.

Chapuis-Lardy, L., Wrage, N., Metay, A., Chotte, J. L. and Bernoux, M. 2006. *Soils, a sink for N_2O? A review*. In press Global Change Biology "Postprint" doi: 10.1111/j.1365–2486.2006.01280.x.

Conen, F. and Neftel, A. 2007. Do increasingly depleted $\delta^{15}N$ values of atmospheric N_2O indicate a decline in soil N_2O reduction? *Biogeochemistry*. DOI: 10.1007/s10533–006–9066-y in press.

Conen, F. and Smith, K. A. 1998. A re-examination of closed flux chamber methods for the measurement of trace gas emissions from soils to the atmosphere. *European J Soil Sci.* **49**(4), 701–707.

Dalsgaard, T., Dezwart, J., Robertson, L. A., Kuenen, J. G. and Revsbech, N. P. 1995. Nitrification, denitrification and growth in artificial thiosphaera-pantotropha biofilms as measured with a combined microsensor for oxygen and nitrous-oxide. *Fems Microbiol. Ecol.* **17**(2), 137–147.

Davidson, D. A. 1991. Fluxes of nitrous oxide and nitric oxide from terrestrial ecosystems. In: *Microbial production and consumption of greenhouse gases: Methane, nitrogen oxides and halomethanes* (eds. J. E. Rogers, and W. B. Whitman). American Society for Microbiology, Washington, D.C., pp. 219–235.

Dobbie, K. E. and Smith, K. A. 2003. Nitrous oxide emission factors for agricultural soils in Great Britain: the impact of soil water-filled pore space and other controlling variables. *Global Change Biol.* **9**(2), 204–218.

Edwards, G. C., Thurtell, G. W., Kidd, G. E., Dias, G. M. and Wagner-Riddle, C. 2003. A diode laser based gas monitor suitable for measurement of trace gas exchange using micrometeorological technique. *Agric. Forest Meteorol.* **115**, 71–89.

Ekschmitt, K., Liu, M. Q., Vetter, S., Fox, O. and Wolters, V. 2005. Strategies used by soil biota to overcome soil organic matter stability - why is dead organic matter left over in the soil?. *Geoderma* **128**(1–2), 167–176.

Flechard, C. R., Neftel, A., Jocher, M. and Ammann, C. 2005. Bidirectional soil-atmosphere N_2O exchange over two mown grassland systems with contrasting management practices. *Global Change Biol.* **11**, 2114–2127.

Flechard, C. R., Neftel, A., Jocher, M., Ammann, C., Leifeld, J. and co-authors. 2007. Temporal changes in soil pore space CO_2 concentration and storage under permanent grassland. *Agricultural and Forest Meteorology* **142**, 66–84.

Galbally, I. E. and Johansson, C. 1989. A model relating laboratory measurements of rates of nitric oxide production and field measurements of nitric oxide emissions from soils. *J Geophys. Res.* **94**(D5), 6473–6480.

Galloway, J. N., Dentener, F. J., Capone, G., Boyer, E. W., Howarth, R. W. and co-authors 2004. Nitrogen cycles, past, present and future. *Biogeochemistry* **70**, 153–226.

Granli, T. and Bockman, O. C. 1994. Nitrous oxide from agriculture. *Norwegian J Agric. Sci. Suppl.* **12**, 1–128.

Gut, A., Blatter, A., Fahrni, M., Lehmann, B. E., Neftel, A. and co-authors. 1998. A new membrane tube technique (METT) for continuous gas measurements in soils. *Plant And Soil* **198**(1), 79–88.

Gut, A., Neftel, A., Staffelbach, T., Riedo, M. and Lehmann, B. E. 1999. Nitric oxide flux from soil during the growing season of wheat by continuous measurements of the NO soil-atmosphere concentration gradient: A process study. *Plant And Soil* **216**(1–2), 165–180.

Hojberg, O., Revsbech, N. P. and Tiedje, J. M. 1994. Denitrification in soil aggregates analyzed with microsensors for nitrous-oxide and oxygen. *Soil Sci. Soc. America J.* **58**(6), 1691–1698.

Houghton, J. T., Meira Filho, L. G., Callander, B. A., Harris, N., Kattenberg, A. and co-authors. 1996. Climate Change 1995; *The Science of Climate Change*. Cambridge University Press, New York.

Leahy, P., Kiely, G. and Scanlon, T. M. 2004 : Managed grasslands: A greenhouse gas sink or source? *Geophys. Res. Lett.* **31**, L20507, doi:10.10292004GL0211161.

Manucharova, N. A., Stepanov, A. L. and Umarov, M. M. 2001. Microbial transformation of nitrogen in water-stable aggregates of various soil types. *Eurasian Soil Sci.* **34**(10), 1125–1131.

Meixner, F. X., Fickinger, T., Marufu, L., Serca, D., Nathaus, F. J. and co-authors. 1997. Preliminary results on nitric oxide emission from a southern African savanna ecosystem. *Nutrient Cycling In Agroecosystems* **48**(1–2), 123–138.

Millington, R. J. 1959. Gas diffusion in porous media. *Science* **130**(3367), 100–102.

Murray, P., Ostle, N., Kenny, C. and Grant, H. (2004). Effect of defoliation on patterns of exudation from *Agrostis Capillaris*. *J. Plant. Nutr. Soil Sci.* **167**, 487–493.

Nannipieri, P., Ascher, J., Ceccherini, M. T., Landi, L., Pietramellara, G. and co-authors.2003. Microbial diversity and soil functions. *European J Soil Sci.* **54**, 655–670.

Neftel, A., Blatter, A., Schmid, M., Lehmann, B. and Tarakanov, S. V. 2000. An experimental determination of the scale length of N_2O in the soil of a grassland. *J Geophys. Res.-Atmos.* **105**(D10), 12095–12103.

Nelson, D. D., Shorter, J. H., McManus, J. B. and Zahniser, M. S. 2002. Sub-part-per-billion detection of nitric oxide in air using a thermoelectrically cooled mid-infrared quantum cascade laser spectrometer. *Applied Phys. B-Lasers Opt.* **75**(2–3), 343–350.

Papen, H. and Butterbach-Bahl, K. 1999. A 3-yr continuous record of nitrogen trace gas fluxes from untreated and limed soil of a N-saturated spruce and beech forest ecosystem in Germany - 1. N2O emissions. *J Geophys. Res.-Atmos.* **104**(D15), 18487–18503.

Parkin, T. B. 1987. Soil microsites as a source of denitrification Variability. *Soil Sci. Soc. America J.* **51**(5), 1194–1199.

Pihlatie, M., Rinne, H. J. I., Pilegaard, K., Dorsey, J. R., Rannik, Ü. and co-authors. 2005. Nitrous oxide emissions from a beech forest floor measured by eddy covariance and soil enclosure techniques. *Biogeosciences* **2**, 377–387.

Potter, C. S., Matson, P. A., Vitousek, P. M. and Davidson, E. A. 1996. Process modelling of controls on nitrogen trace gas emissions from soils worldwide. *J. Geophys. Res.-Atmos.* **101**(D1), 1361–1377.

Rappoldt, C. 1995. Measuring the millimeter-scale oxygen diffusivity in soil using microelectrodes. *European JSoil Sci.* **46**(2), 169–177.

Rappoldt, C. and Crawford, J. W. 1999. The distribution of anoxic volume in a fractal model of soil. *Geoderma* **88**(3–4), 329–347.

Rosenkranz, P., Brüggemann, N., Papen, H., Xu, Z., Seufert, G. and co-authors.2005. N_2O, NO and CH_4 exchange and microbial N turnover over a Mediterranean pine in forest soil. *Biogeosci. Discuss.* **2**, 673–702.

Rothman, L. S., Barbe, A., Benner, D. C., Brown, L. R., Camy-Peyret, C. and co-authors 2003. The HITRAN molecular spectroscopic database: edition of 2000 including updates through 2001. *J Quantitative Spectrosc. & Radiat. Transfer* **82**(1–4), 5–44.

Ryden, J. C. 1981. N_2O exchange between a grassland soil and the atmosphere. *Nature* **292**(5820), 235–237.

Schmid, M., Neftel, A., Riedo, M. and Fuhrer, J. 2001. Process-based modelling of nitrous oxide emissions from different nitrogen sources in mown grassland. *Nutrient Cycling In Agroecosystems* **60**(1–3), 177–187.

Schüssler, W. 1996. *Effektive Parameter zur Bestimmung des Gasaustauschs zwischen Boden und Atmosphäre*, University of Heidelberg, Heidelberg.

Sextone, A. J., Reysbech, N. P., Parkin, T. P. and Tiedje, J. M. 1985. Direct measurements of oxygen profiles and denitrification rates in soil clods. *Soil Sci. Soc. America J.* **49**, 646–651.

Sierra, J., Renault, P. and Valles, V. 1995. Anaerobiosis in saturated soil aggregates: Modelling and experiment. *European J Soil Sci.* **46**(4), 519–531.

Smith, K. A. 1977. Soil Aeration. *Soil Sci.* **123**, 284–291.

Smith, K. A., Clayton, H., McTaggart, I. P., Thomson, P. E., Arah, J. R. M. and co-authors. 1995. The measurement of nitrous-oxide emissions from soil by using chambers. *Philosophical Transactions Of The Royal Society Of London Series A-Mathematical Physical And Engineering Sciences* **351**(1696), 327–337.

Smith, K. A., McTaggart, I. P., Dobbie, K. E. and Conen, F. 1998. Emissions of N_2O from Scottish agricultural soils, as a function of fertilizer N. *Nutrient Cycling In Agroecosystems* **52**(2–3), 123–130.

Spirig, C., Neftel, A., Ammann, C., Dommen, J., Thielmann, A. and co-authors. 2005. Eddy covariance flux measurements of biogenic VOCs during ECHO 2003 using proton transfer reaction mass spectrometry. *Atmos. Chem. Phys.* **5**, 465–481.

Webb, E. K., Pearman, G. I. and Leuning, R. 1980. Correction of Flux Measurements for Density Effects Due to Heat and Water-Vapor Transfer. *Quarterly Journal of the Royal Meteorological Society* **106**, 85–100.

Wienhold, F. G., Welling, M. and Harris, G. W. 1995. Micrometeorological measurement and source region analysis of nitrous-oxide fluxes from an agricultural soil. *Atmos. Environ.* **29**(17), 2219–2227.

Williams, E. J., Hutchinson, G. L. and Fehsenfeld, F. C. 1992. NO and N_2O emission from soil. *Global Biogeochem. Cycles* **13**, 31–46.

Yoshida, N. and Toyoda, S. 2000. Constraining the atmospheric N_2O budget from intramolecular site preference in N_2O isotopomers. *Nature* **405**, 330–334.

Zumft, W. G. 1997. Cell biology and molecular basis of denitrification. *Microbiol. Mol. Biol. Rev.* **61**(4), 533–616.